Eur. Phys. J. B **24**, 23–35 (2001)

THE EUROPEAN PHYSICAL JOURNAL B

EDP Sciences

Quantum computation based on magic-angle-spinning solid state nuclear magnetic resonance spectroscopy

Shangwu Ding[1,2,4,a], C.A. McDowell[3], Chaohui Ye[1,2], Mingsheng Zhan[1,2], Xiwen Zhu[1,2], Kelin Gao[1,2], Xianping Sun[1,2], Xi-An Mao[1,2], and Maili Liu[1,2]

[1] National Laboratory of Magnetic Resonance and Atomic and Molecular Physics, PO Box 71010, Wuhan, Hubei 430071, PR China
[2] Wuhan Institute of Physics and Mathematics, The Chinese Academy of Sciences, PO Box 71010, Wuhan, Hubei 430071, PR China
[3] Department of Chemistry, University of British Columbia, 2036 Main Mall, Vancouver, British Columbia, Canada, V6T 1Z1
[4] Department of Chemistry, National Sun Yat-Sen University, Kaohsiung, Taiwan 807, ROC

Received 19 April 2001

Abstract. Magic-angle spinning (MAS) solid state nuclear magnetic resonance (NMR) spectroscopy is shown to be a promising technique for implementing quantum computing. The theory underlying the principles of quantum computing with nuclear spin systems undergoing MAS is formulated in the framework of formalized quantum Floquet theory. The procedures for realizing state labeling, state transformation and coherence selection in Floquet space are given. It suggests that by this method, the largest number of qubits can easily surpass that achievable with other techniques. Unlike other modalities proposed for quantum computing, this method enables one to adjust the dimension of the working state space, meaning the number of qubits can be readily varied. The universality of quantum computing in Floquet space with solid state NMR is discussed and a demonstrative experimental implementation of Grover's search is given.

PACS. 03.67.-a Quantum information – 76.60.-k Nuclear magnetic resonance and relaxation

1 Introduction

As early as the late 1950's, Landauer and Bennet *et al.* [1–6], investigated the effects of physical laws on computing, such as the reversibility of a computing operation and the minimal energy required to transmit a bit of information. Feynman [7], on the other hand, was studying the fundamental limitations of quantum mechanics on the capacity of (classical) computers. The most important question in these works was what would it happen if computing logic is not presumably given but rather determined by physical laws, particularly, quantum mechanical laws? With the rapid development of very large scale integrated circuitry technology, above question seemed to become important in the early 1980's; that can be rephrased as, what would it happen if the chip size were made so small that one chip contains very few, even just one impurity electron? That background of scientific development initiated quantum computing research. However, quantum computing was basically dormant in the decade of the 1980's. It has since gained increasing attention once the power of a hypothetical quantum computer was revealed, particularly, through the works of Deutsch [8–12] Shor [13,15], Lloyd [16] etc. Deutsch [8,9,12] showed that genuine and massive parallelism can be achieved. Lloyd [16] proposed a quantum computing prototype that has subsequently been followed. Shor [13] demonstrated the power of quantum computer in solving the famous and all-important problem in number theory and public key cryptography system, *i.e.* the prime factoring of large integers. Shor *et al.* [14,15,17], Gottesman [18,19], Steane [20–22], Schumacher [26]and Preskill [23] and others invented a variety of quantum error correction schemes that are crucial to the realization of long-time quantum computing.

Since then, theoretical publications have appeared with increasing frequency, encompassing almost every aspect of computing theory(for review, see, *e.g.*, [27,28]). Remarkable progress in experimental implementation and model proposals also has been made in utilizing an extensive repertoire of sophisticated experimental techniques including atomic interferometry [29], quantum electrodynamic cavity [30–34], ion trap [35,36], polarized photons [37], nuclear spins embedded in an electron system in the quantum Hall regime [38], quantum dots [39], Josephson junction [40], electrons in liquid helium [41], nuclear spins in doped silicon devices [42], single Cooper pair [43], Rydberg atom [44] and liquid NMR [45–61]. Differing from other techniques, the NMR prototype uses bulk samples hence an ensemble of nuclear spins

[a] e-mail: ding@mail.nsysu.edu.tw

rather than pure quantum mechanical systems. Among the above experimental prototypes, NMR is certainly the most promising, to date: all above methods except NMR can only simulate a single quantum logic gate such as controlled NOT gate, but NMR can do much more than that, *e.g.*, it can simulate a quantum network such as the performing of simple arithmetic operations, and a quantum computer that can execute simple quantum algorithms [48–51,53,56,59]. The NMR method offers the first realizable quantum computer operating with more than two qubits, thus providing for the first time a quantum computer with error correction capacity [60]. All these demonstrations used liquid state NMR spectroscopy because of its natural high resolution. While the progress has been remarkable, one severe difficulty with the NMR quantum computer is the exponential loss of the signal sensitivity with the increase of spin numbers (hence usable qubits) in the working molecule. It is clear that establishing an NMR quantum computer with a capacity of over ten qubits is rather challenging [62], if not impossible even though a host of sensitivity-enhancing techniques are available [47].

In this paper, we present an alternative, probably more advantageous, method for performing NMR quantum computing, that is, quantum computing based on solid state NMR involving rotating samples at an angle of 54.74°, the magic-angle to the applied magnetic field. This so-called magic-angle spinning (MAS) [63,64] NMR can be well formulated using Floquet theory [65–74]. From the point of view of quantum computing, the Floquet description offers a method to augment the state space, almost infinitely. In practice, nevertheless, the size of the space is restricted by the signal sensitivity. However, as shown in our theoretical analysis elaborated below, this size can be easily made much larger than that realizable in liquid NMR studies. For quadrupolar nuclei, the sidebands produced by the rotating polycrystalline samples can be as many as thousands or even more [75,76], meaning usable qubits can be easily achieved, even in excess of 10 merely by using conventional NMR techniques, although in this case, the manipulation of quantum states and coherences is more complicated than for spin-1/2 systems. The other obvious advantage of solid state NMR is that the number of spins in a sample is usually much larger than in a liquid sample of the same size, meaning a significant sensitivity gain. Our paper is arranged as follows. In the Section 2, the theory underlying quantum computing with solid state MAS NMR is described; this is the foundation of the subsequent sections of paper and future work. Particularly important are the definition of the pseudo pure state in Floquet space and its connection with quantum computing. While the theoretical framework applies to nuclear spin-1/2 systems as well as to quadrupolar nuclear spins, the remainder of the paper will focus on spin-1/2 systems with chemical shift interactions. Section 3 establishes the correspondence between a pseudo pure state and its spectral representation. This is essential to the read-out function in NMR quantum computing because the directly detectable signals in NMR arise from the single quantum coherences. The theoretical derivation of the spectral signal is demonstrated in Appendix A. The preparation of pseudo pure state is crucial to quantum computing and this is discussed in Section 4. Three different methods are considered. Section 5 analyzes the universality of MAS solid state NMR quantum computing. In Section 6 is demonstrated the implementation of an important quantum computing algorithm, namely, Grover's search, on a solid state NMR quantum computer. The major points of this paper are summarized in the final section.

2 Quantum computing in Floquet space

2.1 Quantum Floquet theory of solid state NMR

A periodic time-dependent Hamiltonian such as that for a nuclear spin system in a polycrystalline sample undergoing rotation at the magic-angle in a static magnetic field is best described employing Floquet theory. Here we summarize the well-developed theory from the perspective of MAS NMR and its significance to quantum computing. Most generally, the evolution of the density matrix, $\rho(t)$, of a spin system can be written as

$$\rho(t) = \hat{T}\mathrm{e}^{-\mathrm{i}\int_0^t \mathrm{d}t' H(t')}\rho(0)\mathrm{e}^{\mathrm{i}\int_0^t \mathrm{d}t' H(t')}. \tag{2.1}$$

It follows, therefore, that evaluating the evolution operator $U(t) = \hat{T}\mathrm{e}^{-\mathrm{i}\int_0^t \mathrm{d}t' H(t')}$ is a central part of spectral lineshape calculations. The straight-forward procedure is to use the multi-step method which divides the time interval, $(0, t_\mathrm{c})$, where t_c is the period of the Hamiltonian, into N equal steps and then one calculates each step by approximating its Hamiltonian as being time-independent

$$U(t) = \mathrm{e}^{-\mathrm{i}H(t_n)\Delta t}...\mathrm{e}^{-\mathrm{i}H(t_i)\Delta t}...\mathrm{e}^{-\mathrm{i}H(0)\Delta t}, \tag{2.2}$$

where $t = nt_\mathrm{c}/N$. This usually involves the diagonalization of each instantaneous Hamiltonian $H(t_i)$. Floquet formalism [67–74], on the other hand, focuses the calculation of the evolution operator on computing the Floquet Hamiltonian H_F by introducing Floquet states $|rn\rangle$ where r is the state index of H and n is the mode index [67,68]

$$\langle pm|H_\mathrm{F}|qn\rangle = h_{pq}^{m-n} + n\omega_\mathrm{c}\delta_{pq}\delta_{mn} \tag{2.3}$$

where h_{pq}^k are the Fourier components of the time-dependent Hamiltonian

$$H_{pq} = \sum_k h_{pq}^k \mathrm{e}^{\mathrm{i}k\omega_\mathrm{c}t}. \tag{2.4}$$

The evolution operator then can be calculated from the following expression

$$\begin{aligned} U_{pq}(t) &= \sum_{n=-\infty}^{\infty} \left\langle pn|\mathrm{e}^{-\mathrm{i}H^\mathrm{F}t}|q0\right\rangle \mathrm{e}^{\mathrm{i}n\omega_\mathrm{c}t}, \\ &= \sum_r \sum_{n,k=-\infty}^{\infty} \left\langle pn\left|\lambda_r^0\right\rangle \left\langle\lambda_r^0\right| qk\right\rangle \mathrm{e}^{-\mathrm{i}(q_r - n\omega_\mathrm{c})t} \end{aligned} \tag{2.5}$$

where the index r runs over the Hilbert space defined by H. For the sake of generality, the Hamiltonian is assumed to be anisotropic, *i.e.* $H \equiv H(\alpha, \beta, \gamma, t)$ where α, β and γ are the Euler angles describing the interaction tensors relative to the laboratory frame (they can be set to zero for solution NMR cases). $|\lambda_r^n\rangle$ and λ_r^n are the eigenstate and eigenvalues of the Floquet Hamiltonian, respectively

$$H^{\mathrm{F}}|\lambda_r^n\rangle = \lambda_r^n|\lambda_r^n\rangle \tag{2.6}$$

$$q_r = \lambda_r^n - n\omega_{\mathrm{c}}. \tag{2.7}$$

Equation (2.5) can be rewritten as [66–68]

$$U(t) = P(t)\mathrm{e}^{-\mathrm{i}Qt}P(0)^{-1} \tag{2.8}$$

where Q is traceless and diagonal with diagonal elements q_r, and $P(t)$ the Floquet amplitude is defined as

$$P_{pq}^n = \left\langle pn|\lambda_q^0\right\rangle \cdot \tag{2.9}$$

At first sight, the estimated magnitude of $U(t)$ can be made almost exact because the values of t can be chosen in arbitrarily small increments. However, in most realistic cases, the Floquet Hamiltonian H_{F} cannot be solved exactly: it requires the use of a perturbation expansion, or equivalently, matrix diagonalization. As has been shown, the order of the expansion series, or the chosen dimension of H_{F} presents a bound to the accuracy of $U(t)$.

If we further define density matrices, observable operators and evolution operators in the Floquet basis, a formalized Floquet theory [77] can be formulated. Specifically, we define

$$U^{\mathrm{F}}(t) = \sum_{n,m} U_{n-m}(t)\,|n\,\rangle\langle\,m|\,\mathrm{e}^{-\mathrm{i}n\omega_{\mathrm{r}}t} \tag{2.10}$$

where $U_n(t)$ are given by

$$U(t, t_0) = \sum_n U_n(t)\mathrm{e}^{-\mathrm{i}n\omega_{\mathrm{r}}t_0}. \tag{2.11}$$

Then the density matrix can be found as

$$\begin{aligned}\sigma(t) &= \sum_{n,m} \left\langle n\left|\sigma^{\mathrm{F}}(t)\right|m\right\rangle \mathrm{e}^{-\mathrm{i}(n-m)\omega_{\mathrm{r}}t} \\ &= \sum_{n,m} \left\langle n\left|U^{\mathrm{F}}\sigma^{\mathrm{F}}(0)U^{\mathrm{F}^{-1}}\right|m\right\rangle \mathrm{e}^{-\mathrm{i}(n-m)\omega_{\mathrm{r}}t}\end{aligned} \tag{2.12}$$

where σ^{F} satisfies the Liouville equation

$$\frac{\mathrm{d}\sigma^{\mathrm{F}}(t)}{\mathrm{d}t} = -\mathrm{i}[H^{\mathrm{F}}, \sigma^{\mathrm{F}}(t)] \tag{2.13}$$

and the initial density matrix at time $t = 0$ is given by

$$\left\langle n\left|\sigma^{\mathrm{F}}\right|m\right\rangle = \delta_{n,m}\sigma(0). \tag{2.14}$$

The observable operator is defined as

$$A^{\mathrm{F}} = \sum_{n,m} A_{n-m}|n\rangle\langle m| = \sum_{n,m} A_m|n\rangle\langle n-m| \tag{2.15}$$

where A_n are the Fourier components of $A(t)$:

$$A(t) = \sum_n A_n\mathrm{e}^{-\mathrm{i}n\omega_{\mathrm{r}}t}. \tag{2.16}$$

Note that definition of the Floquet Hamiltonian H^{F} in the original work [77] is different from equation (2.3). The formalized form of the detection observable D then is easily found from the requirement

$$S(t) = \mathrm{Tr}[D\sigma(t)] = \mathrm{Tr}\left[\tilde{D}^{\mathrm{F}}\sigma^{\mathrm{F}}(t)\right] \tag{2.17}$$

to be

$$\begin{aligned}\tilde{D}^{\mathrm{F}} &= \sum_{n,m} D|n\rangle\langle m|\mathrm{e}^{-\mathrm{i}(n-m)\omega_{\mathrm{r}}t} \\ &= \sum_{n,m} D|n\rangle\langle n+m|\mathrm{e}^{-\mathrm{i}m\omega_{\mathrm{r}}t}.\end{aligned} \tag{2.18}$$

Because of its unified and has a concise form, the formalized Floquet theory will be used throughout the work.

2.2 Floquet pseudo pure state

With the above formalized Floquet theory, the pseudo pure state or effective pseudo pure state introduced by Cory *et al.* [46] can be extended to Floquet space as follows:

$$\Psi^{\mathrm{F}} = \frac{(1-\alpha)\hat{\mathbf{I}} + \alpha\left|\phi^{\mathrm{F}}\right\rangle\left\langle\phi^{\mathrm{F}}\right|}{2^{nk}} \quad (|\alpha| \leq 1) \tag{2.19}$$

where n is the number of spin-1/2 nuclei, k is the (effective) dimension of the "mode" space and $\hat{\mathbf{I}}$ is the identity spinor whose matrix form is an $nk \times nk$ identity square matrix. It is easy to verify that the above definition of the pseudo pure state satisfies the three criteria given by Cory *et al.* [46]: *i.e.*, Ψ^{F} defines a pure density matrix and *vice versa*; Ψ^{F} evolves according to the same unitary transform governing the evolution of a pure density matrix and the measurement value of an observable operator over Ψ^{F} and that of the same observable operator over a pure density matrix differ in a trivial constant only. Therefore, the pseudo pure state in Floquet space can be used to "emulate" quantum computing.

To specify the Floquet space, in the following sections we will focus on the chemical shift interaction. The Euler angles system is defined as follows: the principal axis direction of the chemical shift tensor in the rotor systems is determined with (α, β, γ) while the rotor system is specified by $(\omega_{\mathrm{r}}t, \theta, 0)$ relative to the laboratory frame, where ω_{r} is the sample spinning speed. The most interesting case in solid state NMR as well in this work is when the sample spins at the "magic angle", *i.e.* the spinning axis is tilted $\beta = \beta_m = 54.74°$ with respect to the static magnetic field, which is called magic-angle-spinning(MAS). The chemical shift interaction Hamiltonian then can be

written as [63,64]

$$H_{\rm CS} = -I_z\Big\{\delta_0 + \delta P_2(\cos\theta)\left[\mathrm{P}_2(\cos\beta) - \frac{\eta}{2}\sin^2\beta\cos 2\gamma\right] + \frac{\sqrt{3}}{2}\delta\xi(t)\Big\} \quad (2.20)$$

where δ_0 is the isotropic chemical shift plus the RF offset, δ, η are the anisotropy and asymmetry parameters of the chemical shift tensor, respectively. Denote the three principal values of the chemical shift tensor as $\sigma_{11}, \sigma_{22}, \sigma_{33}$ and assume the convention $\sigma_{11} \geq \sigma_{22} \geq \sigma_{33}$, then there are relations $\delta_0 = \frac{1}{3}(\sigma_{11}+\sigma_{22}+\sigma_{33}), \delta = \sigma_0 - \sigma_{33}, \eta = (\sigma_{11}-\sigma_{22})/\delta$. It is noteworthy that at the magic angle, all the anisotropic terms in equation (2.20) disappear, meaning registered spectra are free from line broadening caused by chemical shift interactions. This is the most important principle in high resolution solid state NMR. The time-dependent term $\xi(t)$ in equation (2.20) is given by

$$\xi(t) = C_1\cos(\omega_{\rm r}t) + S_1\sin(\omega_{\rm r}t) + C_2\cos(2\omega_{\rm r}t) + S_2\sin(2\omega_{\rm r}t) \quad (2.21)$$

where

$$\begin{aligned}
C_1 &= \frac{1}{2}\sin 2\theta\sin\beta[-\cos\beta(\eta\cos 2\gamma + 3)\cos\alpha + \eta\sin 2\gamma\sin\alpha] \\
S_1 &= \frac{1}{2}\sin 2\theta\sin\beta[\cos\beta(\eta\cos 2\gamma + 3)\sin\alpha + \eta\sin 2\gamma\cos\alpha] \\
C_2 &= \frac{1}{2}\sin^2\theta\Big\{\left[\frac{3}{2}\sin^2\beta - \frac{\eta}{2}\cos 2\gamma(1+\cos^2\beta)\right]\cos 2\alpha \\
&\quad + \eta\cos\beta\sin 2\gamma\sin 2\alpha\Big\} \\
S_2 &= \frac{1}{2}\sin^2\theta\Big\{\left[-\frac{3}{2}\sin^2\beta - \frac{\eta}{2}\cos 2\gamma(1+\cos^2\beta)\right]\sin 2\alpha \\
&\quad + \eta\cos\beta\sin 2\gamma\cos 2\alpha\Big\}. \quad (2.22)
\end{aligned}$$

From equations (2.20, 2.21), the Floquet Hamiltonian $H^{\rm F}_{\rm CS}$ can readily be found from equations (2.3, 2.4) [71].

$$\begin{aligned}
\langle 0n\,|H^{\rm F}_{\rm CS}|\,0n\rangle &= n\omega_{\rm r} - \frac{1}{2}\delta\omega \\
\langle 1n\,|H^{\rm F}_{\rm CS}|\,1n\rangle &= n\omega_{\rm r} + \frac{1}{2}\delta\omega \\
\langle 0n\,|H^{\rm F}_{\rm CS}|\,0n\pm 1\rangle &= -\frac{\sqrt{3}}{4}\delta_{\rm CS}C_1 \\
\langle 1n\,|H^{\rm F}_{\rm CS}|\,1n\pm 1\rangle &= \frac{\sqrt{3}}{4}\delta_{\rm CS}C_1 \\
\langle 0n\,|H^{\rm F}_{\rm CS}|\,0n\pm 2\rangle &= -\frac{\sqrt{3}}{4}\delta_{\rm CS}C_2 \\
\langle 1n\,|H^{\rm F}_{\rm CS}|\,1n\pm 2\rangle &= \frac{\sqrt{3}}{4}\delta_{\rm CS}C_2. \quad (2.23)
\end{aligned}$$

All the other elements are zero. The chemical shift interaction is a typical "inhomogeneous" interaction, *i.e.*, it's Hamiltonian at different times is always commutable rendering it unnecessary to perform the time ordering operation in the calculation of the unitary evolution operator. This is a very important property that helps one analyse the evolution of (pseudo pure) quantum states and simplify the design of quantum computing gates. Other important inhomogeneous interactions include the electric quadrupolar interaction and heteronuclear dipolar coupling which will be discussed in future work.

From above paragraphs, some important implications of the applications of Floquet space and solid state NMR to quantum computing in Floquet formalism are summarized as follows: First, Floquet space is dimensionally adjustable, *i.e.*, changing the sample spinning speed $\omega_{\rm r}$ can augment or reduce the effective dimension of the space meaningful for quantum computing. Moreover, contrary to a usual quantum mechanical system, its dimension is not necessarily a power of 2. Second, in solid state NMR quantum computing, the Hamiltonian hence the "operation" can be controlled both with the RF field and sample spinning speed, which provides more flexibility than solution NMR quantum computing. Third, opposite to solution NMR quantum computing which is not satisfactory at low temperatures (below the melting point of the sample used), solid state NMR is usually more sensitive at temperatures as low as possible.

3 Spectral representation of Floquet state

3.1 Signal readout

One of the most essential functions of computing is that the output can be read out. In this section, we give an operational procedure on how to "read out" a pseudo pure state of a solid state NMR quantum computer. In line with standard NMR spectroscopy which measures the induction voltage caused by the transverse magnetization vector of the spin ensemble, this is done by observing the spin ensemble (which is in a pseudo pure state). There are numerous "read" pulses available, but for simplicity and without losing generality, we use single 90° pulse in this work (This is sufficient for chemical shift interaction but for quadrupolar interaction an effective observation may demand more complicated pulses, which will be discussed in the future).

The energy levels of a spin-1/2 system in spinning solid NMR are labeled as shown in Figure 1A. The first index is spin angular momentum quantum number and the second one the mode. The readout function of an output state is given in Figure 1B. Therefore, the FID (free induction decay) signal of a pseudo pure state $|pm\rangle$ can be given as

$$S^{pm}_{+}(t) = \mathrm{Tr}\left[\tilde{I}^{\rm F}_{+}U^{\rm F}_{\rm CS}U^{\rm F}_{90}\sigma^{{\rm F}pm}{U^{\rm F}_{90}}^{-1}{U^{\rm F}_{\rm CS}}^{-1}\right] \quad (3.1)$$

where $U^{\rm F}_{\rm CS}$ and $U^{\rm F}_{90}$ are the Floquet evolution operators corresponding to chemical shift interaction and the 90° pulse, respectively. $\sigma^{{\rm F}pm} \equiv |pm\rangle\langle pm|$ is a pure state in

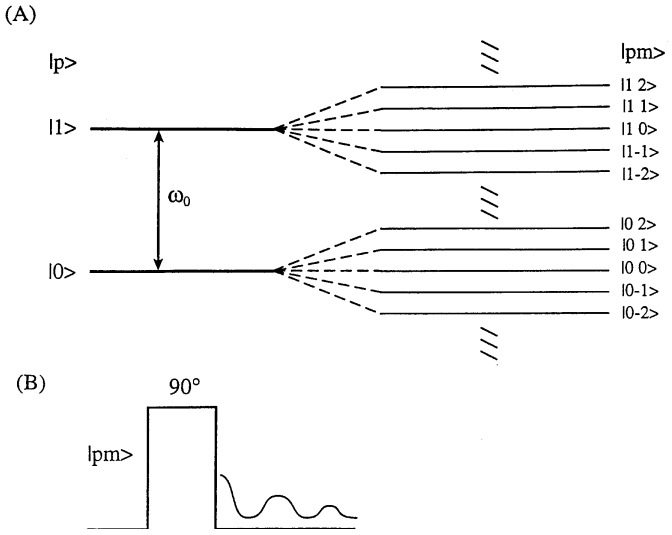

Fig. 1. (A) The Floquet energy levels of spin-1/2 under MAS. (B) The read pulse (90°) for a Floquet state.

Floquet space. $\tilde{I}_+^{\mathrm{F}}$ is the observable operator defined by

$$\tilde{I}_\alpha^{\mathrm{F}} = \sum_{m,n} |n\rangle I_\alpha \langle n+m| \mathrm{e}^{\mathrm{i}m\omega_{\mathrm{r}}t} \quad \alpha = x, y, \pm, \text{etc.} \tag{3.2}$$

3.2 The expressions for U_{90}^{F} and $U_{\mathrm{CS}}^{\mathrm{F}}$

We assume the 90° pulse is along the -x direction in the rotating frame, the RF Hamiltonian is written as

$$H_{\mathrm{rf}} = \omega_1 I_x \equiv \frac{\omega_1}{2}\sigma_x \tag{3.3}$$

where ω_1 is the RF field strength and σ_x is the Pauli matrix. Above equation leads to the following Floquet Hamiltonian

$$\begin{aligned} H_{\mathrm{rf}}^{\mathrm{F}} &= \omega_1 \sum_n |n\rangle I_x \langle n| + n\omega_{\mathrm{r}} \mathbf{1} |n\rangle\langle n| \\ &= \omega_1 \frac{1}{2}\sigma_x \bigoplus \frac{1}{2}\sigma_x \bigoplus \ldots \frac{1}{2}\sigma_x + n\omega_{\mathrm{r}}\mathbf{1}|n\rangle\langle n|. \end{aligned} \tag{3.4}$$

The general expression for the evolution operator of the RF interaction is then given by

$$U_{\mathrm{rf}}^{\mathrm{F}}(t_p) = \mathrm{e}^{-\mathrm{i}H_{\mathrm{rf}}^{\mathrm{F}}t_p} = \mathrm{e}^{-\mathrm{i}[\omega_1 \sum_n |n\rangle I_x \langle n| + n\omega_{\mathrm{r}}\mathbf{1}|n\rangle\langle n|]t_p} \tag{3.5}$$

where t_p is the pulse width. In explicit matrix form, equation (3.5) is

$$U_{\mathrm{rf}}^{\mathrm{F}}(t_p) = \begin{pmatrix} \ddots & & & & \\ & U_{I_x}\mathrm{e}^{-\mathrm{i}\omega_{\mathrm{r}}t_p} & & & \\ & & U_{I_x} & & \\ & & & U_{I_x}\mathrm{e}^{\mathrm{i}\omega_{\mathrm{r}}t_p} & \\ & & & & \ddots \end{pmatrix}. \tag{3.6}$$

If the effective dimension of the mode space is K and the condition $K\omega_{\mathrm{r}}t_p \to 0$ is satisfied, above equation is reduced to

$$U_{\mathrm{rf}}^{\mathrm{F}}(t_p) = \begin{pmatrix} \ddots & & & & \\ & U_{I_x} & & & \\ & & U_{I_x} & & \\ & & & U_{I_x} & \\ & & & & \ddots \end{pmatrix} \tag{3.7}$$

which is a useful simplified expression. The explicit expression of the evolution operator of chemical shift interaction Hamiltonian can be found from equations (2.20–2.22). Specifically, for a spin-1/2 system, from the Hamiltonian equation (2.20), we have

$$\begin{aligned} U_{\mathrm{CS}}(t,t_0) &= \mathrm{e}^{-\mathrm{i}\int_{t_0}^{t} \mathrm{d}t(\omega_{\mathrm{CS}}+\delta_0)I_z} \\ &= \sum_n A_n \mathrm{e}^{-\mathrm{i}(\delta_0+n\omega_{\mathrm{r}})(t-t_0)I_z} \\ &= \sum_n A_n \begin{pmatrix} \mathrm{e}^{-\mathrm{i}[\frac{n\omega_{\mathrm{r}}}{2}(t+t_0)+\frac{\delta_0 t}{2}]} & 0 \\ 0 & \mathrm{e}^{\mathrm{i}[\frac{n\omega_{\mathrm{r}}}{2}(t-3t_0)+\frac{\delta_0 t}{2}]} \end{pmatrix} \mathrm{e}^{\mathrm{i}n\omega_{\mathrm{r}}t_0}. \end{aligned} \tag{3.8}$$

Where the expansion coefficients A_n can be found to be $A_n = |F_n|^2$ with [64]

$$F_n = \frac{1}{2\pi}\int_0^{2\pi} \mathrm{d}\phi\, \mathrm{e}^{\mathrm{i}\left[-n\phi+\frac{C_1}{\omega_{\mathrm{r}}}\sin\phi-\frac{S_1}{\omega_{\mathrm{r}}}\cos\phi+\frac{C_2}{2\omega_{\mathrm{r}}}\sin 2\phi-\frac{S_2}{2\omega_{\mathrm{r}}}\cos 2\phi\right]}. \tag{3.9}$$

Comparing equation (3.8) with equation (2.11), we have

$$U_{\mathrm{CS}n}(t) = A_n \begin{pmatrix} \mathrm{e}^{-\mathrm{i}\left[\frac{n\omega_{\mathrm{r}}}{2}(t+t_0)+\frac{\delta_0 t}{2}\right]} & 0 \\ 0 & \mathrm{e}^{\mathrm{i}\left[\frac{n\omega_{\mathrm{r}}}{2}(t-3t_0)+\frac{\delta_0 t}{2}\right]} \end{pmatrix} \tag{3.10}$$

which, when $t_0 = 0$ is chosen, is reduced to

$$U_{\mathrm{CS}n}(t) = A_n \begin{pmatrix} \mathrm{e}^{-\mathrm{i}\frac{\delta_0+n\omega_{\mathrm{r}}}{2}t} & 0 \\ 0 & \mathrm{e}^{\mathrm{i}\frac{\delta_0+n\omega_{\mathrm{r}}}{2}t} \end{pmatrix} \tag{3.11}$$

which can, in terms of its matrix elements, be denoted in a more concise form as follows

$$U_{\mathrm{CS}n}^{pp}(t) = A_n \mathrm{e}^{-\mathrm{i}\frac{\epsilon_p(\delta_0+n\omega_{\mathrm{r}})t}{2}} \quad p = 0, 1 \tag{3.12}$$

where $p = 0(1)$ corresponds to spin state $|0\rangle = |+\frac{1}{2}\rangle$ $\left(|1\rangle = |-\frac{1}{2}\rangle\right)$ and $\epsilon_p = p - \delta_{p,0}$ with $\delta_{p,0}$ the Kronecker function.

3.3 The effects of U_{90}^{F} and $U_{\mathrm{CS}}^{\mathrm{F}}$ on pseudo pure state

Suppose we have prepared a pseudo pure state $|pm\rangle$ by state labeling techniques [45,46,52] (detailed in Sect. 4

for solid state NMR quantum computing). The effect of the 90° RF pulse on the state is

$$|pm\rangle \rightarrow \sum_{n,l} \mathrm{e}^{-\mathrm{i}n\omega_{\mathrm{r}}t_p}|n\rangle U^{90x}_{n-l}\langle l|pm\rangle = \sum_{n} \mathrm{e}^{-\mathrm{i}n\omega_{\mathrm{r}}t_p}|n\rangle U^{90x}_{n-m}|p\rangle\cdot \quad (3.13)$$

Because the only non-zero component of U^{90x}_n is U^{90x}_0 and notice that $|0\rangle \xrightarrow{90^\circ_x} (|0\rangle + \mathrm{i}|1\rangle)/\sqrt{2}$, $|1\rangle \xrightarrow{90^\circ_x} (|1\rangle + \mathrm{i}|0\rangle)/\sqrt{2}$, the above equation is simply

$$|pm\rangle \xrightarrow{90^\circ_x} \frac{1}{\sqrt{2}}|m\rangle(|p\rangle + \mathrm{i}|p-\epsilon_p\rangle). \quad (3.14)$$

The effect of the chemical shift interaction on a pseudo pure state can be found as follows

$$|pn\rangle \xrightarrow{H^{\mathrm{F}}_{\mathrm{CS}}} U^{\mathrm{F}}_{\mathrm{CS}}|pn\rangle = \sum_{k,l} \mathrm{e}^{-\mathrm{i}k\omega_{\mathrm{r}}t} U_{\mathrm{CS}k-l}|k\rangle\langle l|pn\rangle = \sum_{k} \mathrm{e}^{-\mathrm{i}k\omega_{\mathrm{r}}t} U_{\mathrm{CS}k-n}|pk\rangle\cdot \quad (3.15)$$

The combined effects of the RF pulse and the chemical shift interaction are therefore given as

$$U^{\mathrm{F}}_{\mathrm{CS}}U^{\mathrm{F}}_{90x}|pm\rangle = \frac{1}{\sqrt{2}}\sum_{k} \mathrm{e}^{-\mathrm{i}k\omega_{\mathrm{r}}t} U_{\mathrm{CS}k-m}(|pk\rangle + \mathrm{i}|p-\epsilon_p k\rangle). \quad (3.16)$$

Equations (3.14–3.16) are the basic equations important to the calculations in the following sections.

3.4 The spectral representation of the readout signal

The signal equation (3.1) can be decomposed into two terms $S^{pm}_{+}(t) = S^{pm}_{x}(t) + \mathrm{i}S^{pm}_{y}(t)$ where $S^{pm}_{x}(t), S^{pm}_{y}(t)$ are obtained from equation (3.1) by replacing $\tilde{I}_{+}$ with $\tilde{I}_x$ and $\tilde{I}_y$, respectively. We will give the results here (the derivation of $S^{pm}_{y}(t)$ is shown in Appendix A and it equally applies to the calculation of $S^{pm}_{x}(t)$).

$$S^{pm}_{y}(t) = \mathrm{i}\frac{1}{2}\sum_{k} A_{k-m}\epsilon_p \left[\mathrm{e}^{-\mathrm{i}\epsilon_p(k-m)\omega_{\mathrm{r}}t} - \mathrm{e}^{\mathrm{i}\epsilon_p(k-m)\omega_{\mathrm{r}}t}\right] \quad (3.17)$$

whose spectrum is obtained by Fourier transformation

$$I^{pm}_{y}(\omega) = \mathrm{i}\frac{1}{2}\sum_{k} A_{k-m}\epsilon_p[\delta(\omega - \epsilon_p(k-m)\omega_{\mathrm{r}}) - \delta(\omega + \epsilon_p(k-m)\omega_{\mathrm{r}}). \quad (3.18)$$

For a given system, the largest mode number is fixed, say, K, which is restricted by the sensitivity limit. Then the above equation means that the sideband manifold consists of the following bands: $[-K-m, -K-m+1, ..., K-m]\epsilon_p$ and $[-K+m, -K+m+1, ..., K+m]\epsilon_p$. The amplitude of each band depends on the value of p: for different p, there is a 180° phase factor difference. Therefore, a unique one-to-one correspondence is established between a pseudo pure state and a spectral representation. The signal $S^{pm}_{y}(t)$ (or $I^{pm}_{y}(\omega)$) contains two groups of bands with opposite signs in intensity. If quadrature detection is used, the signal is found to be

$$S^{pm}_{+}(t) = \sum_{k} A_{k-m}\epsilon_p \mathrm{e}^{-\mathrm{i}\epsilon_p(k-m)\omega_{\mathrm{r}}t} \quad (3.19)$$

and its spectrum is readily found to be

$$I^{pm}_{y}(\omega) = \sum_{k} A_{k-m}\epsilon_p \delta(\omega - \epsilon_p(k-m)\omega_{\mathrm{r}}) \quad (3.20)$$

which contains only one group of sidebands given by indices $[-K+m, -K+m+1, ..., K+m]\epsilon_p$. As a demonstration, we choose the six-level system shown in Figure 2 in which $|K| = 1$. Then the spectral representations of all the pseudo pure states are given in Figure 3 and Figure 4 for single crystal and powder samples, respectively. The one-to-one correspondence between state and spectrum is

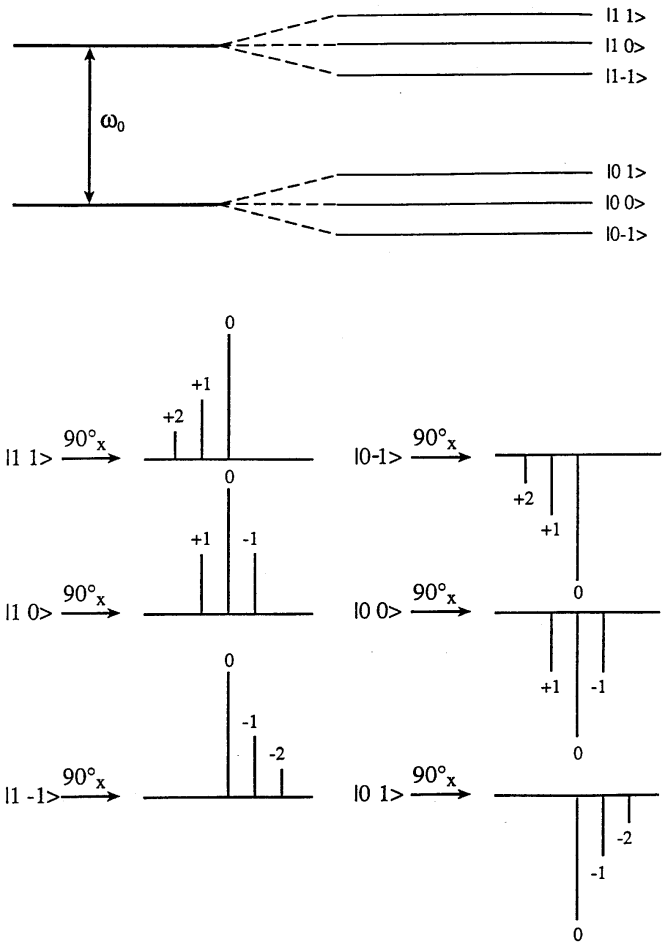

Fig. 2. Upper: the sub-manifold of six energy levels of a spin-1/2 system under MAS and lower: the representation of each state.

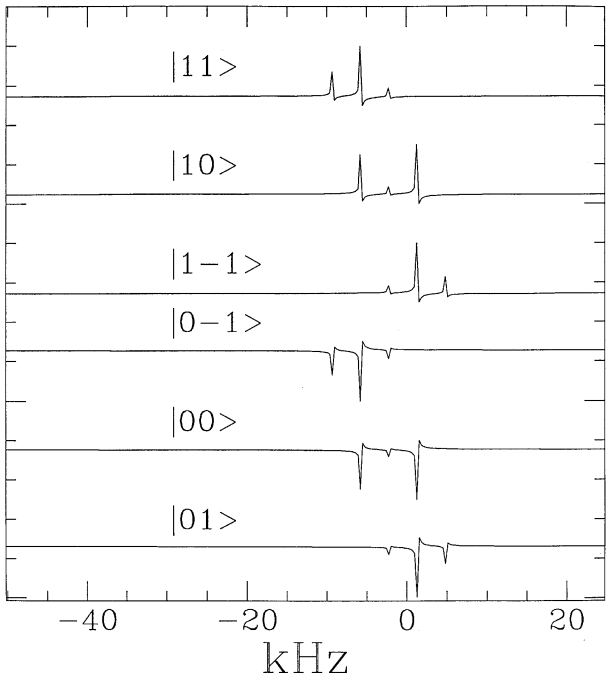

Fig. 3. The readouts of the Floquet system shown in Figure 2 for a single crystal sample. The parameters are $\delta_{\rm CS} = 20$ kHz, $\eta_{\rm CS} = 0.5$, the spinning speed $\omega_{\rm r} = 4$ kHz. The relative orientation of the crystal with respect to the magnetic field is described by two Euler angles (between the lab frame and the principal axis system of the CSA tensor) $(\alpha, \beta) = (30°, 60°)$.

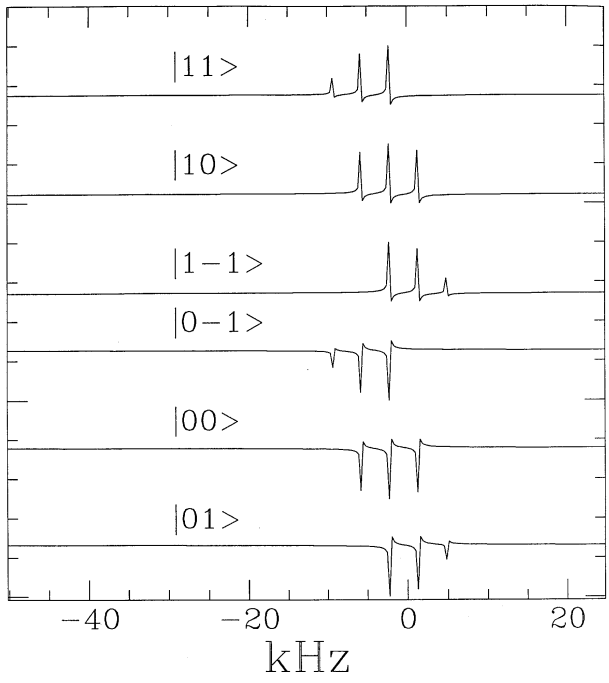

Fig. 4. The readouts of the Floquet system shown in Figure 2 for real polycrystalline powder sample. The parameters: $\delta_{\rm CS} = 20$ kHz, $\eta_{\rm CS} = 0.5$ and spinning speed $\omega_{\rm r} = 4$ kHz.

obvious. The pseudo states are differentiated by amplitude distribution or by a phase factor or both. The spectra are absorptive for powder sample but for single crystal, they may be dispersive but in the later case, the relative phase differences can still be used to unambiguously identify the particular pseudo pure state of the solid state NMR quantum computer before the readout RF pulse was applied.

4 State labeling

4.1 General

State labeling is the unique feature of ensemble quantum computing because a pure state is not naturally available in an ensemble. To carry out quantum computation, one must first "purify" the ensemble so that it can be regarded as being in a pure state. The problem of state labeling in solution NMR has been well addressed. There are two types of labeling: one is temporal and another spatial. The former uses proper time averaging and the latter uses spatial averaging, of the density matrices, to construct a pseudo pure state. Here we show how these methods can be extended to Floquet space quantum computing.

Given an initial density matrix, $\rho^{\rm F}(t_0)$, state labeling renders it a pseudo pure state and a quantum computation task can be undertaken starting from it as follows

$$P^{\rm F} U^{\rm F} \rho^{\rm F}(t_0) U^{{\rm F}^{-1}} = C \left|\phi_0^{\rm F}\right\rangle\!\left\langle\phi_0^{\rm F}\right| = c\psi^{\rm F} \qquad (4.1)$$

where C is the computation operator and c is a constant coefficient and $P^{\rm F}$ a certain preparation (not unitary in most cases).

State labeling from the initial (thermal state) density matrix given by $\langle n|\sigma^{\rm F}(0)|m\rangle = \sigma(0)\delta_{0,m}\delta_{0,n}$ is a trivial task because there are only two non-zero terms for spin-1/2 systems. Either with phase cycling (two experiments) or by applying a gradient field, a specified state can be chosen using the routine techniques. However, this is not the general case because, first, the initial density matrix in formalized Floquet theory can be chosen as a different form $\langle n|\sigma^{\rm F}(0)|m\rangle = \sigma(0)\delta_{m,n}$ and secondly, state labeling may need to start with a density matrix other than the thermal equilibrium form. In addition, certain computations may require a pure state with the mode indices not equal to zero. Therefore, in the following two general techniques will be given which can be employed for any type of mixed state.

4.2 Multi-pulse techniques

From Section 3, a pure state corresponds to certain peak profile in an MAS spectrum. The preparation of a pseudo pure state, therefore, is equivalent to constructing a subspectrum with specific peak profile. Over the past decades, there have been developed an array of techniques in solid state NMR to manipulate the MAS spectral peaks, such as TOSS (total suppression of sidebands), PASS (phase

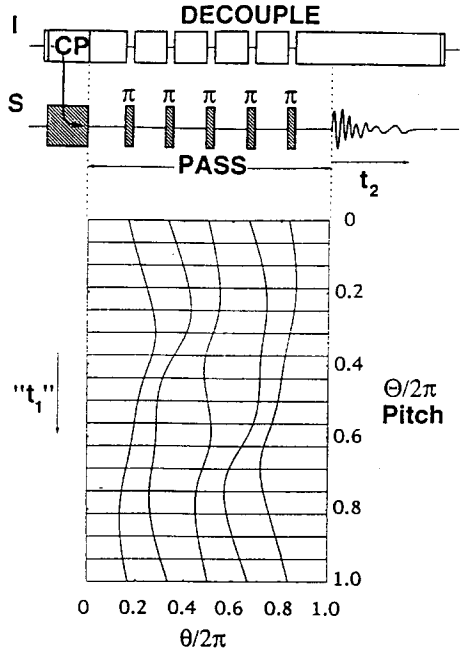

Fig. 5. The pulse sequence of a 2D PASS experiment for spin-1/2 systems proposed by Atzutkin *et al.* [79] [ASL].

adjusted spinning sidebands), IRS (isotropic rotation sequence) and their combinations and two-dimensional extensions etc. [78]. As an example, we demonstrate that the 2D-PASS sequence is a satisfactory technique for state labeling. The sequence consists of five π pulses and is shown in Figure 5. The parameter Θ (pitch) is used to characterize the separations between each adjacent pair of π pulses. In 2D-PASS experiment [79], Θ also represents the first dimension and it is changed systematically according to prescribed separations between pulse pairs such as

$$2\sum_{q=1}^{n}(-1)^q e^{im\theta_q} + 1 - (-1)^n e^{im(\Theta+\theta_T)} = 0$$

$$-2\sum_{q=1}^{n}(-1)^{n+q}\theta_q + \theta_T = 0$$

$$\theta_T = 0 \quad (4.2)$$

where n is the total number of the sidebands in the MAS spectrum. The meaning of other parameters is shown in Figure 5. Each sideband (or central band) can be extracted from the projection along the first dimension. When necessary, the intensity of each band can be modified by adding a pair of pulse $90^\circ_{-x}\theta_x$ at the end of the PASS sequence, where the value of θ is determined by the desired intensity of the band. The peak profile of a pseudo pure state can then be constructed by adjusting Θ and θ_x systematically. For example, given a peak profile $A_K, K = 1, 2, ..., n$ where A_K is the intensity of Kth sidebands. The second dimension signal (FID) in a 2D-PASS experiment is given by

$$S(t_2) = \sum_{k=-\infty}^{\infty} a^{(k)} e^{-ik\Theta} e^{i(\delta_0 + k\omega_r)t_2} \quad (4.3)$$

where the explicit expression of $a^{(k)}$ can be found in reference [77]. The simplest peak "basis" can be chosen as

$$\sum_{\Theta} S^{\Theta}(t_2) x_K^{\Theta} = A_K e^{i(\delta_0 + K\omega_r)t_2} \quad (4.4)$$

where x_K $(= \sin\theta_x)$ are to be determined. By summing all possible values of Θ the above equation can be simplified as

$$\sum_{\Theta} a^{(k)} e^{ik\Theta} x_K^{\Theta} = \delta_{kK} A_k. \quad (4.5)$$

Therefore, the values of x_K can be found out by solving the above linear equations

$$x = A^{-1}\Delta \quad (4.6)$$

where the matrices $A = a^{(k)}e^{ik\Theta}$ and $\Delta = \delta_{kK}A_K$. It can be easily verified that A^{-1} exists.

Therefore, any subspectral profile can be constructed with this sequence: $90^\circ_x - [ASL] - 90^\circ_x - \theta_{-x}$. The number of the values of Θ is determined by the number of the sidebands in the MAS spectrum and in principle there are no restrictions on the values of Θ. Therefore, this technique can readily deal with a system with as many as hundreds or even thousands of sidebands.

To reduce the number of steps to a practically acceptable level, the density matrix may be simplified before the standard state labeling techniques is invoked. We believe that the selective excitation techniques such as Dante pulse sequence [80], can be incorporated in the preparation of the density matrix for state labeling.

4.3 Gradient field selection

Temporal labeling methods as discussed above are easy to implement and retain the sensitivity of the whole sample, but usually require a number of experiments. This reduces computing efficiency and in the least-promising cases might conceal the advantage of quantum parallelism [45,48]. Therefore, temporal labeling is best suitable for low-qubit implementations. Another technique, *i.e.*, spatial labeling was proposed by Cory *et al.* [46,52] which may or may not use phase cycling. Here this method is extended to the solid state MAS NMR case.

In a magnetic gradient field, the Floquet energy levels are dispersed along the direction of gradient. The effect of a gradient field on the energy levels is the same as in normal Hilbert space. Without losing generality, we consider the case where the gradient field is along the z-direction (parallel with the static magnetic field). We use the "sandwich" pulse sequence $G_{z1}(t_{G1}) - 90^\circ_x - G_{z2}(t_{G2})$ where t_{G1}, t_{G2} are the gradient pulse lengths and 90° is the RF pulse, as shown in Figure 6. The evolution operator during

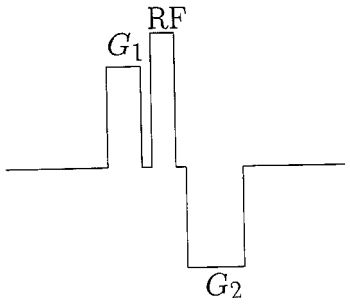

Fig. 6. The typical pulse arrangement for state labeling with gradient field selection.

the gradient pulse can be from equation (2.11)

$$U_G(t,t_0) = \mathrm{e}^{-\mathrm{i}zG_z\int_{t_0}^{t}\mathrm{d}t(\omega_{\mathrm{CS}}(t)+\delta_0)I_z} = \sum_n A_n \begin{pmatrix} \mathrm{e}^{-\mathrm{i}zG_z\left[\frac{n\omega_{\mathrm{r}}}{2}(t+t_0)+\frac{\delta_0 t}{2}\right]} & 0 \\ 0 & \mathrm{e}^{\mathrm{i}zG_z\left[\frac{n\omega_{\mathrm{r}}}{2}(t-3t_0)+\frac{\delta_0 t}{2}\right]} \end{pmatrix} \times \mathrm{e}^{\mathrm{i}n\omega_{\mathrm{r}}t_0} = \sum_n U_{G\,n}(t)\mathrm{e}^{\mathrm{i}n\omega_{\mathrm{r}}t_0} \quad (4.7)$$

from which the evolution operator in Floquet space can be easily found using equation (2.10).

With any given initial state $\rho^{\mathrm{F}}(t_0)$, the final density matrix after the sandwich pulse sequence is given by

$$\rho^{\mathrm{F}}(t) = U^{\mathrm{F}}_{G2}(t_2,t_0^{'})U^{\mathrm{F}}_{90x}U^{\mathrm{F}}_{G1}(t_{G1},t_0)\rho^{\mathrm{F}}(t_0){U^{\mathrm{F}}_{G1}}^{-1} \times (t_{G1},t_0){U^{\mathrm{F}}_{90x}}^{-1}{U^{\mathrm{F}}_{G2}}^{-1}(t_2,t_0^{'}) \quad (4.8)$$

where $t_2 = t_{G2} + t_0^{'}, t_0^{'} = t_0 + t_{G1} + t_p$. It is easy to show that above equation only provides a constraint on the the Floquet space if the gradient field is time independent. Using equation (2.10), we can find the condition for state labeling from equation (4.8) as

$$\epsilon_p k\omega_{\mathrm{r}}G_{z2}t_{G2} + \epsilon_q l\omega_{\mathrm{r}}G_{z1}t_{G1} = 0 \quad (4.9)$$

where k, l are integers. The detailed derivation of above equations is given in Appendix B. By setting G_{z1}, G_{z2}, t_{G1} and t_{G2} properly, the desired situation that only one term survives the pulse sequence can be realized, thus a pseudo pure state is prepared.

Obviously, the gradient field method can also be incorporated with selective excitation but its merit is unknown. In the following, we will focus on the techniques that do not need a gradient. The thorough investigation of the application of a gradient field in solid state NMR quantum computing will be presented elsewhere.

5 Universality and gate design

The above procedures for implementing state labeling can be extended to construct basic operating matrices, *i.e.*, elementary quantum logic gates. The universality can be ensured if all possible operations can be realized with a set of elementary gates. The central problem is how to realize the operations that transform any state into any other state. As an example, we show that the 2D-PASS sequence can be used as a basic pulse block in constructing universal logic gates. From "peak manipulation" point of view, if all peak profiles can be realized starting from any peak profile, the gates thus constructed are universal.

Here we give a general discussion on the relationship between peak manipulation and the construction of complete unitary transform (universal gates). Starting from the initial density matrix $\rho^{\mathrm{F}}(0)$, two pseudo pure states can be prepared as follows

$$\begin{aligned} \rho_1^{\mathrm{F}} &= P_1^{\mathrm{F}}\rho^{\mathrm{F}}(0) \\ \rho_2^{\mathrm{F}} &= P_2^{\mathrm{F}}\rho^{\mathrm{F}}(0). \end{aligned} \quad (5.1)$$

Thus the unitary transform that maps state ρ_1^{F} to state ρ_2^{F} can be realized with

$$U_{12}^{\mathrm{F}} = P_2^{\mathrm{F}}{P_1^{\mathrm{F}}}^{-1}. \quad (5.2)$$

Suppose there are L Floquet states that are usable for quantum computing where $L = L_d + L_u$ where L_d, L_u are the number of states corresponding to spin quantum number $\frac{1}{2}, -\frac{1}{2}$, respectively. Its is easy to find from the energy levels that the total number of peaks from this energy level manifold is $L-1$. Therefore, for a unitary matrix of $M \times M$ dimension, $M+1$ Floquet states are needed. The unitary matrices can then be determined from the peak manipulation matrices which constitute a complete set:

$$U_{mn}^{\mathrm{F}} = \sum_{i,j} a_{ij}^{mn}P_{ij}^{mn}. \quad (5.3)$$

The unitary matrices thus constructed necessarily form a complete set because peak manipulation matrices are complete.

The experimental realization of the universal operation can be implemented with, *e.g.*, 2D-PASS sequence [ASL] shown in Figure 5. For example, pulse sequence $\theta_x^{(n)} - 90^\circ_{-x} - [ASL]^{-1} - 90^\circ_{-x} - 90^\circ_x - [ASL] - 90^\circ_x - \theta_{-x}^{(m)}$, where $[ASL]^{-1}$ is the time-inverted version of the ASL sequence shown in Figure 5, gives the pulse sequence that transforms a pseudo pure state $|pm\rangle\langle pm|$ to another $|qn\rangle\langle qn|$. With these transform matrices, therefore, any possible operations compatible with the system are realizable.

This method, perhaps rather forceful, is workable in practice, at least for low qubit cases. However, we point out that there may exist more efficient pulse sequences that can realize above transformations and that is to be the major goal of our subsequent efforts.

6 Example: Grover's search

In this section, we demonstrate the use of the theoretical formalism developed in the preceding sections to implement experimentally a quantum algorithm. We will use Grover's search [81] as an example.

Grover's search consists of four steps [81]: (1) the preparation of pseudo pure state; (2) HW transform; (3) conditional flipping; (4) average about the mean; where step (3) and (4) are repeated $2\sqrt{N}/\pi$ times for an N-item search. When using the 2D-PASS sequence, steps (1–3) can be incorporated in one experimental step with the initial density matrix as the input and an equi-amplitude superposed state as the output. In the output state, the phase difference between the flipped bit and the rest is 180°. The step (4) corresponds to the transform matrix with elements $U_{ij} = \frac{1}{2} - \delta_{ij}$, each of which can be implemented according to equation (5.3). Generally, the corresponding pulse sequence can then be designed as follows: $90^\circ_x - [ASL] - 90^\circ_x - \theta^{(l)}_{-x} - \theta^{(m)}_x - 90^\circ_{-x} - [ASL]^{-1} - 90^\circ_x - [ASL] - 90^\circ_x - \theta^{(n)}_{-x} - Acquisition$ with l, m, $n = 1, 2, 3, 4...$ This means the number of experiments is $l \times m \times n$ which would soon become impractically large. However, above construction of the pulse sequence may reduce the number of experiments substantially. For example, for the 2-qubit search experiment demonstrated in this work, however, only four experiments are required for each search. The Floquet energy level diagram and four "working" states are illustrated in Figures 7A and B, respectively.

The experiments were performed on a Bruker MSL-200 NMR spectrometer. The ^{13}C resonance frequency was 50.3 MHz. The sample was hexamethylbenzene (HMB) which was spun at the magic-angle with a spinning speed of 5 kHz. The aromatic carbon atom which has a chemical shift anisotropy of about 100 ppm is the spin we used for quantum computing. The methyl carbon has a small chemical shift anisotropy and its peak is used as the phase standard of the spectra. With the spinning speed used, there are two sidebands that are clearly observable for the aromatic carbon. Based on pulse sequences and the procedures discussed in the previous section, four search results were obtained and are shown in Figure 8. As seen from Figure 7B and Figure 8, the theoretical prediction is in good agreement with the experimental result.

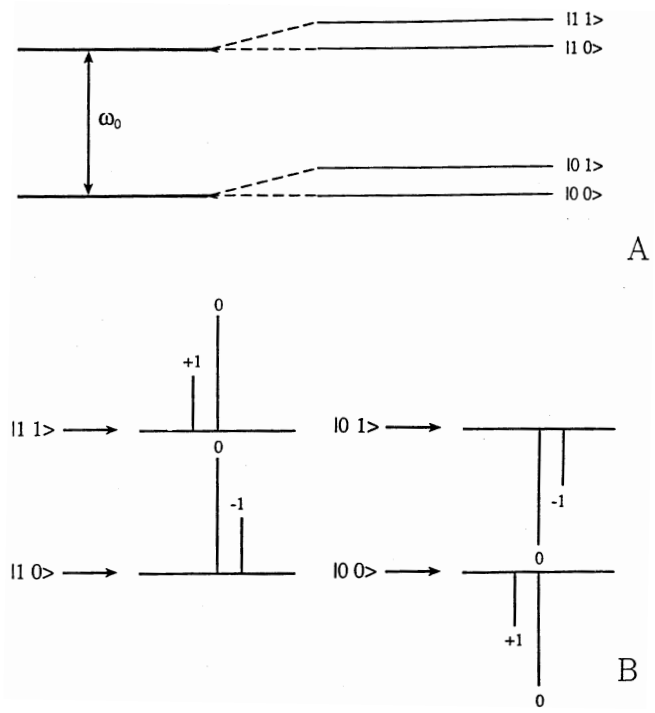

Fig. 7. Grover search based on MAS NMR. (A) Energy level diagram showing the states used for the experiment. (B) Schematic representation of the four Floquet states chosen for the experiment.

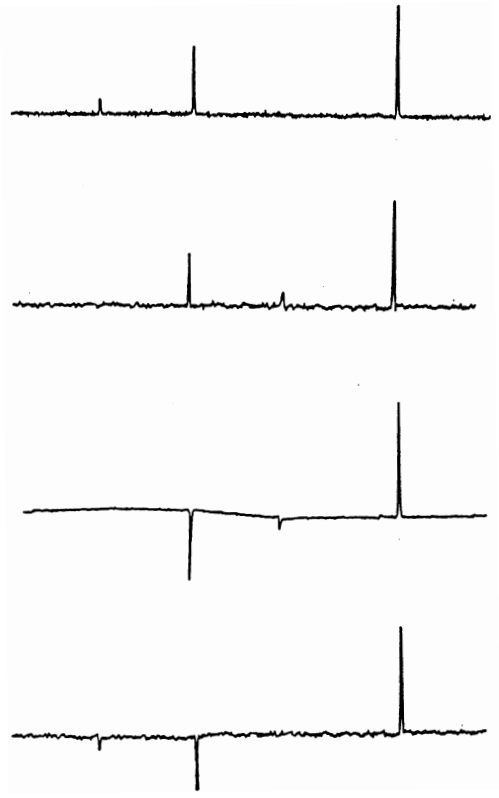

Fig. 8. The experimental result of four possible states with Grover search algorithm based on MAS NMR, represented with the sideband pattern of the aromatic carbons of hexamethylbenzene. The rightmost peak comes from the methyl carbons and is used as phasing reference.

7 Conclusions

In this work, magic-angle spinning solid state NMR QC theory is developed based on formalized Floquet theory. Because the mode space is controlled by the sample spinning speed, the realizable number of qubits is changeable and can be made as large as the task demands (the ultimate limitation comes from signal to noise ratio). The techniques required for state manipulations (labeling, coherence selection etc.) are analyzed. The spectral representations of state is given that is crucial to readout of QC registers. The basic QC gates are demonstrated and an important QC algorithm is shown to be realizable in solid state quantum computer. Based on these theoretical analyses, it has become clear that solid state NMR may become a good alternative methodology for ensemble quantum computing. This technique has many advantages: such as large working space (Floquet) that is adjustable. This makes a vast difference between this technique

and previously proposed NMR-related methods because the dimension of the computing space can be augmented significantly for the spin systems which otherwise can only offer very low number of qubits. The sensitivity is generally higher than its liquid state counterpart of the same size because of the difference in the number densities of nuclear spins. The pulse sequences are conveniently implemented with conventional solid state NMR techniques although non-conventional techniques may be used to enhance sensitivity and achieve higher-qubit operations. We point out that the number of qubits currently manageable in our initial experiment is rather limited mainly because of the brute force pulse sequences used. We believe, however, more efficient pulse sequences for implementing higher-qubit QC operations in Floquet space can be found.

The chemical shift interaction of single spin-1/2 system is exemplified in this work, but the principles and procedures used here can be extended to other interactions such as dipolar and quadrupolar interactions, which is the object of further work. In fact, when more spins are involved in coupled systems or large quadrupolar interaction is present, high qubits are more conveniently realized in those systems. Nevertheless, we recognize that the difficulty involved in manipulating experimentally these systems may be significantly greater.

Finally, for a practical quantum computer, error correction is necessary. The recently published error correction schemes must be modified to accommodate solid state NMR based quantum computing in Floquet space.

This work was supported by the Hundred Talents Program of the Chinese Academy of Sciences and the Natural Science and Engineering Research Council of Canada. SD acknowledges the stimulating discussions with Prof. Guo Wei Wei of the National University of Singapore. He also thanks Dr. Ole N. Antzutkin of the Laboratory of Chemical Physics of the National Institute of Diabetes and Digestive and Kidney Diseases, NIH (USA) for sending a reprint of his review paper [78] on sideband manipulation techniques that are important in experimental implementation of solid state NMR quantum computing.

Appendix A: Derivation of equation (3.17) and equation (3.18)

From equations (3.1, 3.16), the signal $S_y^{pm}(t)$ can be written as

$$S_y^{pm}(t) = \frac{1}{2}\mathrm{Tr}\Big\{ \sum_{k,k'} \mathrm{e}^{-\mathrm{i}k\omega_r t} U_{\mathrm{CS}k-m}(|pk\rangle + |p-\epsilon_p k\rangle) \times \mathrm{e}^{\mathrm{i}k'\omega_r t}(\langle pk'| + |p-\langle \epsilon_p k'|) U^{-1}_{\mathrm{CS}k'-m} \sum_{l,j} |l\rangle I_y \langle l+j| \mathrm{e}^{\mathrm{i}j\omega_r t} \Big\}$$
$$= \frac{1}{2}\mathrm{Tr}\Big\{ \sum_{k,k',j,l} \mathrm{e}^{-\mathrm{i}(k-k'-j)\omega_r t} U_{\mathrm{CS}k-m} \times (|pk\rangle + |p-\epsilon_p k\rangle)(\langle pk'| + \langle p-\epsilon_p k'|) U^{-1}_{\mathrm{CS}k'-m} |l\rangle I_y \langle l+j| \Big\}. \quad (1)$$

In terms of matrix elements, it becomes

$$\begin{aligned} S_y^{pm}(t) &= \frac{1}{2}\sum_{k,k'j,l}\sum_{s,n} \mathrm{e}^{-\mathrm{i}(k-k'-j)\omega_r t} \\ &\quad \times \left(U^{sp}_{\mathrm{CS}k-m} + U^{sp-\epsilon_p}_{\mathrm{CS}k-m}\right)\langle n|k\rangle \\ &\quad \times \sum_{q,n'} \left({U^{pq}_{\mathrm{CS}k'-m}}^{-1} + {U^{p-\epsilon_p\, q}_{\mathrm{CS}k'-m}}^{-1}\right) \\ &\quad \times \langle n'|k'\rangle\langle n'|l\rangle\langle q|I_y|s\rangle\langle l+j|n\rangle \\ &= \frac{1}{2}\sum_{k,k'}\sum_{s,q}\left[U^{sp}_{\mathrm{CS}k-m} + U^{sp-\epsilon_p}_{\mathrm{CS}k-m}\right] \\ &\quad \times \left[{U^{pq}_{\mathrm{CS}k'-m}}^{-1} + {U^{p-\epsilon_p q}_{\mathrm{CS}k'-m}}^{-1}\right] I_y^{qs} \\ &= \frac{1}{2}\sum_{k,k'}\sum_{s,q}\Big[U^{sp}_{\mathrm{CS}k-m}{U^{pq}_{\mathrm{CS}k'-m}}^{-1} \\ &\quad + U^{sp}_{\mathrm{CS}k-m}{U^{p-\epsilon_p q}_{\mathrm{CS}k'-m}}^{-1} + U^{sp-\epsilon_p}_{\mathrm{CS}k-m}{U^{pq}_{\mathrm{CS}k'-m}}^{-1} \\ &\quad + U^{sp-\epsilon_p}_{\mathrm{CS}k-m}{U^{p-\epsilon_p q}_{\mathrm{CS}k'-m}}^{-1}\Big]. \end{aligned} \quad (2)$$

Note that $U_{\mathrm{CS}n}$ is diagonal and I_y is Hermitian and its diagonal elements are all zero. The above equation only has two non-zero terms given as

$$S_y^{pm}(t) = \frac{1}{2}\sum_{k,k'}\Big[U^{pp}_{\mathrm{CS}k-m}{U^{p-\epsilon_p\, p-\epsilon_p}_{\mathrm{CS}k'-m}}^{-1} I_y^{p-\epsilon_p\, p} + U^{p-\epsilon_p\, p-\epsilon_p}_{\mathrm{CS}k'-m}{U^{pp}_{\mathrm{CS}k-m}}^{-1} I_y^{p\, p-\epsilon_p}\Big]. \quad (3)$$

Using the matrix expression of the $U_{\mathrm{CS}n}(t)$ equation (3.12) and the orthogonal properties of Bessel functions contained in coefficients A_n, the time-domain signal equation (3.17) is readily obtained. The calculation of $S_x^{pm}(t)$ is completely the same as given above and its result is

$$S_x^{pm}(t) = \frac{1}{2}\sum_k A_{k-m}\epsilon_p\left[\mathrm{e}^{-\mathrm{i}\epsilon_p(k-m)\omega_r t} + \mathrm{e}^{\mathrm{i}\epsilon_p(k-m)\omega_r t}\right]. \quad (4)$$

The quadrature detection signal (Eq. (3.19)) is the sum of above equation and equation (3.17).

Appendix B: Derivation of equation (4.9)

The effect of a gradient magnetic field is used to select certain orders of coherences from the initial density matrix by spatially averaging out others. An arbitrary element of ρ_0^{F} is denoted as $|pi\rangle\langle qj|$ with coherence order of $p-q$ and $i-j$ in Hilbert and mode space, respectively. To see how gradient field select density matrix elements, we first calculate the following term (see Eq. (4.8))

$$U^{\mathrm{F}}_{G_{z2}}(t_2, t_0^{'})U^{\mathrm{F}}_{90^\circ x}U^{\mathrm{F}}_{G_{z1}}(t_{G1}, t_0)|pi\rangle|qj| \quad (5)$$

which can be written as according to equations (2.10, 3.5)

$$\begin{aligned}
&\sum_{n,m,l,k} U_{G_2 n-m} U^{\mathrm{F}}_{90^\circ x} \\
&\times U_{G_1 l-k} |n\rangle\langle m|l\rangle\langle k|pi|\langle qj| \mathrm{e}^{\mathrm{i}(n-m)\omega_{\mathrm{r}} t} \\
&= \sum_{n,m} U_{G_2 n-m} U^{\mathrm{F}}_{90^\circ x} \\
&\times U_{G_1 m-i} |pm\rangle\langle qj| \mathrm{e}^{\mathrm{i}(n-m)\omega_r t} \\
&= \sum_{n,m} U_{G_2 n-m} E^{-\mathrm{i}[\omega_1 \sigma_{n'} |n'\rangle I_x \langle n'| + n'\omega_{\mathrm{r}} \mathbf{1} |n'\rangle\langle n'|] t_p} \\
&\times U_{G_1 m-i} |pm\rangle\langle qj| \mathrm{e}^{\mathrm{i}(n-m)\omega_{\mathrm{r}} t} \\
&= \sum_{n,n',m} U_{G_2 x} U_{I_x} |n'\rangle\langle n'| \mathrm{e}^{\mathrm{i}n'\omega_{\mathrm{r}} t_p} \\
&\times U_{G_1 m-i} |pm\rangle\langle qj| \mathrm{e}^{\mathrm{i}(n-m)\omega_{\mathrm{r}} t} \\
&= \sum_{n,m} U_{G_2 n-m} U_{I_x} U_{G_1 m-i} |pm\rangle\langle qj| \mathrm{e}^{\mathrm{i}\omega_{\mathrm{r}}(m t_p + (n-m)t} \quad (6)
\end{aligned}$$

where t_p is the 90 degree pulse width and $t = t_2 - t_0$. Assuming $\rho^{\mathrm{F}}(t_0) = |pm\rangle\langle qj|$, equation (4.8) is then written as

$$\begin{aligned}
&\sum_{n,m,n'm'} U_{G_2 n-m} U_{I_x} \\
&\quad \times U_{G_1 m-i} |pm\rangle\langle qm'| U^{-1}_{G_1 m'-j} U^{-1}_{I_x} U^{-1}_{G_2 n'-m'} \\
&\quad \times \mathrm{e}^{\mathrm{i}\omega_{\mathrm{r}}\left[(m-m')t_p + (n-n'+m'-m)t\right]}. \quad (7)
\end{aligned}$$

Let $t_0 = 0$. Using equation (4.7), the terms related to the gradient field in above equation are of the form

$$\begin{aligned}
&\mathrm{e}^{\pm\mathrm{i}\frac{n-m}{2} G_{1z} z \omega_{\mathrm{r}} t}, \mathrm{e}^{\pm\mathrm{i}\frac{m-i}{2} G_{1z} z \omega_{\mathrm{r}} t} \\
&\mathrm{e}^{\pm\mathrm{i}\frac{n'-m'}{2} G_{2z} z \omega_{\mathrm{r}} t}, \mathrm{e}^{\pm\mathrm{i}\frac{m'-j}{2} G_{1z} z \omega_{\mathrm{r}} t}. \quad (8)
\end{aligned}$$

Note that the gradient fields are symmetrical with respect to z axis and the indices n, m, n', m' run from $-\infty$ to ∞. Therefore, above equation would vanish unless

$$(i-j) G_1 t_{G_1} = (n-n') G_2 t_{G_2}. \quad (9)$$

If we denote the coherence orders in the mode space during the first and second gradient field pulses, $i-j$ and $n-n'$, as l and k, respectively, above condition is the same as equation (4.9) by adding the coherence transfer condition in Hilbert space.

References

1. R. Landauer, IBM J. Res. Dev. **5**, 183 (1961).
2. C.H. Bennett, IBM J. Res. Dev. **17**, 525 (1973).
3. C.H. Bennett, Intl. Theo. Phys. **21**, 905 (1982).
4. P. Benioff, Phys. Rev. Lett. **48**, 1581 (1982).
5. E. Fredkin, T. Toffoli, Intl. J. Theo. Phys. **21**, 219 (1982).
6. C.H. Bennett, SIAM J. Comput. **18**, 766 (1989).
7. R.P. Feynman, Opt. News **11**, 11 (1982); Reprinted in Found. Phys. **16**, 507 (1986).
8. D. Deutch, Proc. R. Soc. London A **400**, 97 (1985).
9. D. Deutch, Proc. R. Soc. London, A **425**, 73 (1989).
10. D. Deutch, R. Josza, Proc. R. Soc. London A **439**, 533 (1992).
11. A. Berthiam, D. Deutch, Ro. Jozsa, *Proceedings of the Workshop on Physics and Computer Science – PhysCompu '94* (1994), p. 60.
12. D. Deutch, A. Barenco, A. Ekert, Proc. R. Soc. London, A **449**, 669 (1995).
13. P.W. Shor, *Proceedings of the 35th Annual Symposium on the Foundations of Computer Science*, edited by S. Goldwasser (1994), p. 124.
14. P.W. Shor, Phys. Rev. A **52**, R2493 (1995).
15. A.R. Galderbank, P.W. Shor, Phys. Rev. A **54**, 1098 (1996).
16. S. Lloyd, Phys. Rev. Lett. **75**, 346 (1995).
17. D.P. DiVicenzo, P.W. Shor, Phys. Rev. Lett. **77**, 3260 (1996)
18. D.A. Gottesman, Phys. Rev. A **54**, 1862 (1996).
19. D.A. Gottesman, Phys. Rev. A **57**, 127 (1998).
20. A.M. Steane, Phys. Rev. Lett. **77**, 793 (1996).
21. A.M. Steane, Phys. Rev. A **54** , 4741 (1996).
22. A.M. Steane, Nature, **399**, 124 (1999).
23. J. Preskill, Proc R. Soc. London A **454**, 385 (1998).
24. E. Knill, R. Laflamme, Phys. Rev. A **55**, 900 (1997).
25. E. Knill, R. Laflamme, W.H. Zurek, Proc R. Soc. London A **454**, 265 (1998).
26. B. Schumacher, Phys. Rev. A **51**, 2738 (1995).
27. A. Berenco, Comtemp. Phys. **37**, 3375 (1996).
28. A.M. Steane, Rep. Progr. Phys. **61**, 117 (1998).
29. A. Barenco, D. Deutch, A. Ekert, R. Jozsa, Phys. Rev. Lett. **74**, 20 (1995).
30. Q.A. Turchette, C.J. Hood, W. Lange, H. Mabuchi, H.J. Kimble, Phys. Rev. Lett. **75**, 4710 (1995).
31. T. Sleator, H. Weinfurter, Phys. Rev. Lett. **74**, 4087 (1995).
32. P. Domokos, J.M. Raimond, M. Brune, S. Haroche, Phys. Rev. A **52**, 3554 (1995).
33. T. Pellizzri, S.A. Gardiner, J.I. Cirac, P. Zoller, Phys. Rev. Lett. **75**, 3788 (1995).
34. C. Monroe, D.M. Meekhof, B.E. King, W.M. Itano, D.J. Wineland, Phys. Rev. Lett. **75**, 4714 (1995).
35. J.I. Cirac, P. Zoller, Phys. Rev. Lett. **74**, 4091 (1995).
36. S.R. Jefferts, C. Monroe, E.W. bell, D.J. Wineland, Phys. Rev. **51**, 3112 (1995).
37. P. Törmä, S. Stenholm, Phys. Rev. A **54**, 4701 (1996).
38. V. Privman, I.D. Vagner, G. Keventsel, `quant-ph/9707017`.
39. N.H. Bonadeo, J. Erland, D. Gammon, D. Park, D.S. Katzer, D.G. Steel, Science **282**, 1473 (1998).
40. J.E. Mooij, T.P. Orlando, L. Levitov, L. Tian, C.S. van der Wal, S. Lloyd, Science **285**, 1036 (1999).
41. P.M. Platzman, M.I. Dykman, Science **284**, 1967 (1999).
42. B.E. Kane, Nature **393**, 133 (1998).
43. Y. Nakamura, Yu.A. Pashkin, J.S. Tsai, Nature **398**, 786 (1999).
44. J. Ahn, T.C. Weinacht, P.H. Bucksbaum, Science **287**, 463 (2000).
45. N.A. Gershenfeld, I.L. Chuang, Science **275**, 3350 (1997).
46. D.G. Cory, A.F. Fahmy, T.F. Havel, Proc. Natl. Acad. Sci. USA **94**, 1634 (1997).

47. N.A. Gershenfeld, I.L. Chuang, Science **277**, 1689 (1997).
48. I.L. Chuang, N. Gershenfeld, M. Kubinec, Phys. Rev. Lett. **80**, 3408 (1998).
49. I.L. Chuang, M.K. Vandersypen, X. Zhou, D.W. Leung, S. Lloyd, Nature **393**, 143 (1998).
50. J.A. Jones, M. Mosca, J. Chem. Phys. **109**, 1648 (1998).
51. J.A. Jones, M. Mosca, R.H. Hansen, Nature **393**, 344 (1998).
52. D.G. Cory, M.D. Price, T.F. Havel, Physica D **120**, 82 (1998).
53. I.L. Chuang, N. Gershenfeld, M. Kubinec, D.W. Leung, Proc R. Soc. London A **454**, 447 (1998).
54. N. Linden, H. Barjat, R. Freeman, Chem. Phys. Lett. **296**, 61 (1998).
55. N. Linden, B. Herve, R.J. Carbajo, R. Freeman, Chem. Phys. Lett. **296**, 61 (1998).
56. X. Fang, X.W. Zhu, M. Feng, X. Mao, F. Du, Phys. Rev. A **61**, 002307 (1999).
57. Z.L. Madi, R. Bruschweiler, R.R. Ernst, J. Chem. Phys. **109**, 10603 (1998).
58. M. Marjanska, I.L. Chuang, M.G. Kubinec, J. Chem. Phys. **112**, 5095 (2000).
59. R. Marx, A.F. Fahmy, J.M. Myers, W. Bermel, S.J. Glaser, Phys. Rev. A **62**, 12310 (2000).
60. D.G. Cory, M.D. Price, W.E. Maas, E. Knill, R. Laflamme, W.H. Zurek, T.F. Havel, S.S. Somaroo, Phys. Rev. Lett. **81**, 2152 (1998).
61. A.K. Khitrin, B.M. Fung, J. Chem. Phys. **112**, 6963 (2000).
62. W.S. Warren, Science **277**, 1688 (1997).
63. U. Haeberlen, *High Resolution NMR in Solids: Selective Averaging* (Academic Press, New York, 1976).
64. M. Mehring, *Principles of High Resolution NMR in Solids* (Springer-Verlag, Berlin, 1983).
65. J.H. Shirley, Phys. Rev. B **138**, 979 (1965).
66. M.M. Maricq, Phys. Rev. B **25**, 6622 (1982).
67. Y. Zur, M.H. Levitt, S. Vega, J. Chem. Phys. **78**, 5293 (1983).
68. S. Vega, E.T. Olejniczak, R.G. Griffin, J. Chem. Phys. **80**, 4832 (1984).
69. A. Schmidt, S. Vega, J. Chem. Phys. **87**, 6895 (1987).
70. A. Kubo, C.A. McDowell, J. Chem. Phys. **93**, 7156 (1990).
71. A. Schmidt, S. Vega, J. Chem. Phys. **96**, 2655 (1992).
72. T. Nakai, C.A. McDowell, J. Chem. Phys. **96**, 3452 (1992).
73. S. Ding, C.A. McDowell, Chem. Phys. Lett. **288**, 230 (1998).
74. S. Ding, C.A. McDowell, Mol. Phys. **95**, 841 (1998).
75. H.J. Jakobsen, J. Skibsted, H. Bildsoe, N.C. Nielsen, J. Magn. Reson. **85**, 173 (1989).
76. J. Skibsted, N.C. Nielsen, H. Bildsoe, H.J. Jakobsen, J. Magn. Reson. **95**, 88 (1991).
77. T.O. Levante, M. Baldus, B.H. Meier, R.R. Ernst, Mol. Phys. **86**, 1195 (1995).
78. O.N. Antzutkin, Progr. NMR Spectrosc. **35**, 203 (1999).
79. O.N. Antzutkin, S.C. Shekar, M.H. Levitt, J. Magn. Reson. A **115**, 7 (1995).
80. R.R. Ernst, G. Bodenhausen, A. Wokaun, *Principles of Nuclear magnetic Resonance in One and Two Dimensions* (Claredon, 1987).
81. L.K. Grover, Phys. Rev. Lett. **79**, 325 (1997).